JOURNAL OF GEOPHYSICAL RESEARCH, VOL. 112, B08309, doi:10.1029/2006JB004754, 2007

Decay of aftershock activity for Japanese earthquakes

K. Z. Nanjo,[1] B. Enescu,[2] R. Shcherbakov,[3] D. L. Turcotte,[4] T. Iwata,[5] and Y. Ogata[5]

Received 14 September 2006; revised 26 April 2007; accepted 15 May 2007; published 18 August 2007.

[1] Aftershock decay is often correlated with the modified Omori's law: $dN/dt = \tau^{-1}(1 + t/c)^{-p}$, where dN/dt is the occurrence rate of aftershocks with magnitudes greater than a lower cutoff m, t is time since a mainshock, τ and c are characteristic times, and p is an exponent. Extending this approach, we derive two possibilities: (1) c is a constant independent of m and τ scales with m and (2) c scales with m and τ is a constant independent of m. These two are tested by using aftershock sequences of four relatively recent and large earthquakes in Japan. We first determine for each sequence the threshold magnitude above which all aftershocks are completely recorded and use only events above this magnitude. Then, visual inspection of the decay curves and statistical analysis shows that the second possibility is the better approximation for our sequences. This means that the power law decay of smaller aftershocks starts after larger times from the mainshock. We find a close association of our second result with a solution obtained for a damage mechanics model of aftershock decay. The time delays associated with aftershocks, according to the second possibility, can be understood as the times needed to nucleate microcracks (aftershocks). Our result supports the idea that the c value is a real consequence of aftershock dynamics associated with damage evolution.

Citation: Nanjo, K. Z., B. Enescu, R. Shcherbakov, D. L. Turcotte, T. Iwata, and Y. Ogata (2007), Decay of aftershock activity for Japanese earthquakes, *J. Geophys. Res.*, *112*, B08309, doi:10.1029/2006JB004754.

1. Introduction

[2] It is a remarkable fact that an earthquake of large magnitude is usually followed by a sequence of smaller earthquakes called aftershocks. These aftershocks occur close to the focus of the mainshock, gradually decreasing in activity with increasing time over many months and even years. For a large earthquake, the number of its aftershocks recorded by seismometers reaches several hundreds or more. The behavior of aftershock sequences has been studied statistically and empirically and several laws have been derived [e.g., *Utsu*, 1961; *Kisslinger and Jones*, 1991; *Utsu et al.*, 1995]. Three well-known laws are the Gutenberg-Richter (GR) law, Båth's law, and the modified Omori's law.

[3] The GR frequency-magnitude law [*Gutenberg and Richter*, 1954] is valid for all earthquakes both regionally and globally [*Turcotte*, 1997]. This law is also valid for aftershocks [*Utsu*, 1961, 1962, 1969; *Guo and Ogata*, 1997; *Enescu and Ito*, 2002]. The number N of earthquakes with magnitudes greater than or equal to m is well approximated by the relation

$$\log_{10} N = A - bm, \tag{1}$$

where A and b are constants. The constant b or "b value" is usually in the range $0.8 \leq b \leq 1.2$ [*Turcotte*, 1997]. The constant A is the logarithm of the number of events for $m \geq 0$ in a given sample. The correct estimate of the A and b values depends on the completeness of the sample under investigation. The data completeness can be considered based on a threshold called completeness magnitude m_c, above which all events in the sample can be interpreted to have been recorded. We follow the conventional notation m_c, as this is frequently used in the scientific literature [e.g., *Wiemer and Wyss*, 2000, 2002; *Woessner and Wiemer*, 2005].

[4] Båth's law [*Båth*, 1965] states that the difference in magnitude Δm between a mainshock with magnitude m_{ms} and its largest aftershock with magnitude m_{asmax} ($\Delta m = m_{ms} - m_{asmax}$) is approximately constant with $\Delta m \approx 1.2$. However, in a number of studies on the statistical variability of Δm [*Vere-Jones*, 1969; *Console et al.*, 2003; *Helmstetter and Sornette*, 2003; *Vere-Jones et al.*, 2006; D. Vere-Jones et al., A further note on Bath's law, submitted to *Bulletin of Seismological Society of America*, 2007] it has been argued that this law might be an artifact caused by the different criteria that seismologists apply to define mainshocks and aftershocks.

[5] The third law is the modified Omori's law (or the Omori-Utsu law) that was proposed by *Utsu* [1961]. This law describes the temporal decay of aftershock activity and

[1] Swiss Seismological Service, ETH Zurich, Zurich, Switzerland.
[2] Physics of the Earth, GeoForschungsZentrum, Potsdam, Germany.
[3] Center for Computational Science and Engineering, c/o Department of Physics, University of California, Davis, California, USA.
[4] Department of Geology, University of California, Davis, California, USA.
[5] Institute of Statistical Mathematics, Tokyo, Japan.

0148-0227/07/2006JB004754$09.00

Table 1. List of Main Shocks[a]

Main Shock	Date	Lat., deg.	Long., deg.	Dep., km	m_{ms}	L, km	T, days
Kobe	17 Jan 1995	34.58	135.03	16	7.3	89.3	1000
Tottori	6 Oct 2000	35.27	133.33	9	7.3	89.3	1000
Niigata	23 Oct 2004	37.28	138.87	13	6.8	50.2	378
Fukuoka	20 Mar 2005	33.73	130.17	9	7.0	63.2	225

[a]Date: the occurrence time of the mainshock; Lat.: latitude of the mainshock; Long.: longitude of the mainshock; Dep.: depth of the mainshock; m_{ms}: mainshock magnitude; *L*: linear extent of the space window obtained using the equation of *Kagan* [2002]; *T*: length of the time window.

is given in the form $dN/dt = K(c + t)^{-p}$, where dN/dt is the rate of occurrence of aftershocks with magnitudes greater than or equal to m, t is the time since the mainshock, c is a characteristic time, K is a constant, and p is the exponent called the "p-value." *Omori* [1894] proposed the case of $p = 1$, which is generally a good approximation. No systematic dependence of p on m or m_{ms} has been found [*Utsu*, 1962; *Hamaguchi and Hasegawa*, 1970; *Utsu et al.*, 1995]. This law can be rewritten as [*Shcherbakov et al.*, 2004, 2005, 2006]:

$$dN/dt = \tau^{-1}(1 + t/c)^{-p}, \quad (2)$$

where $\tau = c^p/K$ is a characteristic time. This time can be interpreted as the waiting time for the occurrence of the first aftershock with a magnitude greater than or equal to m in a given aftershock sequence. However, some studies [*Gross and Kisslinger*, 1994; *Narteau et al.*, 2002; *Ben-Zion and Lyakhovsky*, 2006] showed that the aftershock decay rates could also be fitted with an exponential function.

[6] *Shcherbakov et al.* [2004, 2005, 2006] combined the three laws given above to obtain a generalized Omori's law for aftershock decay rates. The main difference from the original form of the modified Omori's law is that c is no longer a constant but scales with the lower cutoff magnitude m. This scaling was tested using the aftershock sequences of five relatively large earthquakes that occurred in California between 1992 and 2004. A fundamental question is whether the scaling of c with m is valid for aftershock sequences in tectonically different regions. The primary objective of the present study is to test this validity, using the four Japanese earthquakes (Table 1). These earthquakes are chosen because of the following reasons: they occurred in the Japanese regions which are tectonically and geographically different from California considered by *Shcherbakov et al.* [2004, 2005, 2006], and these earthquakes are relatively recent with relatively well-documented aftershock sequences.

[7] Theoretical models of seismicity like Epidemic Type Aftershock Sequence (ETAS) consider an earthquake sequence as the result of a cascade of aftershocks triggered by each previous event [e.g., *Guo and Ogata*, 1997; *Ogata*, 1999; *Helmstetter et al.*, 2005; *Hainzl and Ogata*, 2005]. We limit our analysis to a modified-Omori's-law-based approach, rather than including more complex ETAS modeling because this is sufficient to capture the essential aspects of the relaxation process that follows the occurrence of the mainshock. Thus we regard the four large earthquakes (section 3) of this study as mainshocks and assume they are able to produce significant aftershock sequences.

[8] Smaller aftershocks in the early stage of an aftershock sequence are, in many cases, missing from the earthquake catalogs, as they are "masked" by the mainshock coda and overlap each other on the seismograms [*Kagan*, 2004]. For large mainshocks, the failure of observing systems at stations close to the epicenter causes a lowering of the detectability of small events. In such circumstances, the c value may be overestimated. True c values are difficult to estimate accurately unless very careful observations are started immediately after the mainshock. When data are taken from ordinary earthquake catalogs, the estimated c value may partially reflect the effect of the incomplete detection of small aftershocks shortly after the main shock [*Utsu et al.*, 1995]. It is appropriate for our analysis to use only events in magnitude and time windows where aftershocks are unlikely to be missing. Our approach to the effect of missing aftershocks at short times is different from that taken by *Shcherbakov et al.* [2004, 2005, 2006].

[9] The present study pays special attention to many observational and Earth-oriented issues, while focusing on the existence of c, which is still under debate [e.g., *Narteau et al.*, 2002; *Kagan*, 2004; *Shcherbakov et al.*, 2004, 2005, 2006; *Gasperini and Lolli*, 2006; *Lolli and Gasperini*, 2006]. The relevance of the analysis and significance of the results are clearly discussed.

2. Two Hypotheses to Describe Aftershock Decay Rates

[10] We initially follow the approach of *Shcherbakov et al.* [2004, 2005, 2006]. Then we modify their approach to define the scaling of c with m, assuming that τ is a constant independent of m. We also describe another possibility: the scaling of τ with m, assuming that c is a constant independent of m. The two hypotheses are described in detail below.

[11] Integration of equation (2) from $t = 0$ to the time T (>0) gives $N = c\tau^{-1}(p - 1)^{-1}[1 - (1 - T/c)^{1-p}]$ if $p \neq 1$ and $N = c\tau^{-1}\ln(1 + T/c)$ if $p = 1$ where $\ln(x)$ is the natural logarithm of a variable x. We take the former equation with $p \neq 1$ for further analysis. The reader may note that the latter can be used to easily obtain the total number of aftershocks N, since $p = 1$ is a good approximation. However, because it is standard practice to consider a range of p values in modeling the aftershock decay, we use the former equation, with $p \neq 1$ to obtain N.

[12] If equation (2) is assumed to be valid at all times, then the total number N in the limit $T \to \infty$ is finite only for $p > 1$. However, the values of T considered in this work are finite: T is of the order of several hundred days, up to 1000 days. With these values, $T \gg c$ ($\leq$1 day) so that T/c is very large. The number of aftershocks that occur after a time T from the mainshock is very small. Thus for practical purposes, T can be considered as the "lifetime" of our aftershock sequences. Assuming that $T/c \to \infty$ and $p > 1$, we obtain $N = c\tau^{-1}(p - 1)^{-1}$. We substitute this relation

into equation (1) to obtain $c/\tau = (p-1)10^{A_T - b_T m}$, where $b = b_T$ and $A = A_T$ (i.e., b and A values calculated for aftershocks with relative occurrence times $t \leq T$). Up to this point the theoretical development is the same as in the work of *Shcherbakov et al.* [2004, 2005, 2006], except that these authors include the Båth's law [*Båth*, 1965] into their formulations. We do not use the Båth's law in our study since it may be an artifact, as explained in section 1. By using $c/\tau = (p-1)10^{A_T - b_T m}$ and assuming that p is a constant independent of m and $m_{\rm ms}$ [*Utsu*, 1962; *Kisslinger and Jones*, 1991; *Utsu et al.*, 1995], we formulate two new hypotheses.

[13] The first hypothesis is that c is a constant $c = c_0$, independent of m, and τ is dependent on m (hypothesis I). Hence substituting $\tau = \tau(m)$ and $c = c_0$ into $c/\tau = (p-1)10^{A_T - b_T m}$, we get

$$\tau(m) = c_0 (p-1)^{-1} 10^{-A_T + b_T m}. \quad (3)$$

We then use $\tau = \tau(m)$ and $c = c_0$ in equation (2) to obtain

$$dN/dt = \tau(m)^{-1} (1 + t/c_0)^{-p}. \quad (4)$$

At time $t = 0$, the rate is $dN/dt = c_0^{-1}(p-1)10^{AT - bTm}$, a function of m, c_0, and p if b_T and A_T are known parameters.

[14] The second hypothesis is that τ is a constant $\tau = \tau_0$, independent of m, and c scales with m (hypothesis II). Substitution of $\tau = \tau_0$ and $c = c(m)$ into $c/\tau(p-1)10^{A_T - b_T m}$ gives

$$c(m) = \tau_0 (p-1) 10^{A_T - b_T m}. \quad (5)$$

In a similar manner to the first hypothesis, we rewrite equation (2) using $\tau = \tau_0$ and $c = c(m)$,

$$dN/dt = \tau_0^{-1} [1 + t/c(m)]^{-p}. \quad (6)$$

At time $t = 0$, the rate is $dN/dt = 1/\tau_0$, a constant independent of m.

[15] We will examine whether these hypotheses work well to describe the temporal decay of aftershocks for the four cases considered in this study and which is better to describe it. We next introduce the data used for analysis and the selection criterion for the aftershocks.

3. Data and Definition of Aftershocks: Preliminary Analysis of Aftershock Activity

3.1. Aftershock Data

[16] We analyze four aftershock sequences that follow the occurrence of the 1995 Kobe earthquake, the 2000 Western Tottori earthquake, the 2004 Mid Niigata Prefecture earthquake and the 2005 West Off Fukuoka Prefecture earthquake, respectively. We use the seismic catalog maintained by the Japan Meteorological Agency (JMA), which includes hypocentral locations and occurrence times of earthquakes with magnitudes $m_{\rm JMA}$ greater than or equal to 0 since 1923 in and around Japan. This is considered to be one of the most complete and reliable catalogs in the world.

[17] While the seismic catalog we use in this study is reliable, there are several factors which do influence data quality immediately after a mainshock. The most important factors are mentioned at the end of section 1, while a detailed discussion can be found in the work of *Kagan* [2004]. Therefore we have to be careful in evaluating whether the c values reflect the true properties of the aftershock sequences or are solely caused by network issues. We will pay special attention to this issue in section 4.

[18] We basically consider earthquakes of magnitudes greater than or equal to 2.0. The magnitude of 2.0 is thought to be above the lower limit of completeness in the studied regions. The completeness of earthquake data immediately after the mainshocks will be discussed in detail later.

3.2. Temporal and Spatial Windows for the Aftershocks

[19] To identify aftershocks we define a space and time window relative to the mainshock. For the Kobe and Tottori earthquakes we take the time window of $T = 1000$ days after the mainshock as in the analysis of *Shcherbakov et al.* [2004, 2005]. We consider shorter time windows for the recent Niigata and Fukuoka earthquakes: $T = 378$ and $T = 225$, respectively. These shorter windows reflect the time periods for which aftershock data were available when this analysis was carried out. The T-values are tabulated in Table 1.

[20] As the space window we consider a square region centered on the mainshock epicenter with the linear extent L (km). We use the scaling law obtained by *Kagan* [2002], $L = 0.02 \times 10^{0.5 m_{ms}}$, because it is a standard approximation to estimate aftershock areas [*Shcherbakov et al.*, 2004, 2005; *Helmstetter et al.*, 2005]. An important question is whether the results substantially change when the side length of the spatial window varies. We address this question by considering several possible values for this length. Details of the choice of the side-length will be discussed in section 6.

[21] The reader may note that *Kagan* [2002] used the moment-magnitude $m_{\rm w}$, not $m_{\rm JMA}$, to obtain the scaling. However, above $m_{\rm W} = 5.5$, $m_{\rm JMA}$ can be considered statistically equivalent to $m_{\rm W}$, while below $m_{\rm W} = 5.5$, $m_{\rm JMA}$ is smaller than $m_{\rm W}$ [*Scordilis*, 2005]. The magnitudes of the mainshocks in Table 1 are all significantly larger than 5.5. Thus $m_{\rm ms}$ is directly substituted into the equation of *Kagan* [2002] to estimate L.

[22] Depth is also required to define the space window. The four earthquakes discussed in this paper are crustal events and the depth of 20 km is thought to be the lower limit of the seismogenic zone in the studied regions. Thus we consider events with depths shallower than 20 km for all cases.

[23] We first define the aftershocks of the Kobe earthquake. Substituting $m_{\rm ms} = 7.3$ into the equation of *Kagan* [2002], we obtain $L = 89$ km (Table 1). Only the earthquakes inside the space-time window defined by $L = 89$ km and $T = 1000$ days are considered aftershocks. The total number of aftershocks with magnitudes greater than or equal to 2.0 is 1445. The same analysis to define aftershocks has been performed for the other three sequences. The computed lengths L are summarized in Table 1.

3.3. Frequency-Magnitude Distribution

[24] Before testing the two hypotheses, we need to determine $b_{\rm T}$ and $A_{\rm T}$ of each aftershock sequence. The

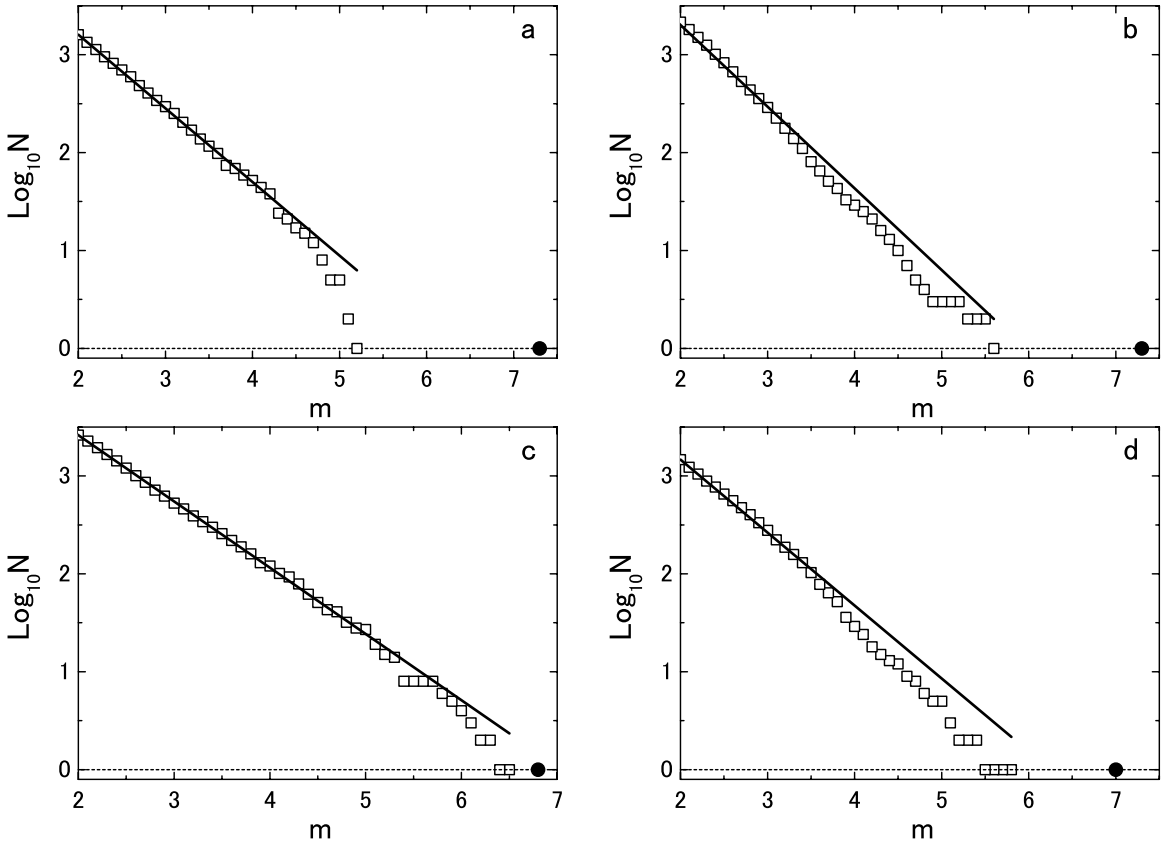

Figure 1. Frequency-magnitude distributions for the aftershocks of (a) 1995 Kobe earthquake; (b) 2000 Western Tottori earthquake; (c) 2004 Mid Niigata Prefecture earthquake and (d) 2005 West Off Fukuoka Prefecture earthquake. Only events occurred within a spatial window of linear size L, centered on the mainshock are considered. The temporal windows are of 1000 days in the case of Kobe and Tottori sequences and of 378 days and 225 days for the Niigata and Fukuoka aftershocks, respectively. Mainshock magnitude (m_{ms}) is shown by a large dot. Also shown in Figures 1a–1d is the GR law fit, with the A_T and b_T values calculated as explained in the text. We use (A_T, b_T) = (4.64, 0.74) for Figure 1a, (4.92, 0.80) for Figure 1b, (4.77, 0.68) for Figure 1c, and (4.66, 0.75) for Figure 1d.

cumulative number of aftershocks N of the 1995 Kobe earthquake is given in Figure 1a as a function of magnitude, m. b_T is estimated using the corrected maximum-likelihood technique [e.g., *Guo and Ogata*, 1997; *Marzocchi and Sandri*, 2003] to have no bias on b value estimation. Note that this correction is not reported in the original *Aki*'s [1965] paper and its modified version by *Shi and Bolt* [1982]. The resulting b_T value is 0.74±0.01 (0.01 shows the standard error). This estimate is computed based on aftershocks with magnitudes above $m = 2.0$. By substituting $b_T = 0.74$, $m = 2.0$, and $N = 1445$ into equation (1) we obtain $A_T = 4.64$. Using the determined b_T and A_T values, we fit a straight line to the data in Figure 1a. We can assume that the GR law holds so that $b_T = 0.74$ and $A_T = 4.64$ are used in equations (3) and (5). We followed the same procedure for the other sequences and the results are summarized in Table 2.

3.4. Magnitude Versus Time From Mainshock

[25] The distinct magnitude-time pattern in the early part of an aftershock sequence can be seen conveniently if one plots the aftershock magnitude versus the logarithm of the time $\log_{10}(t)$ after the mainshock [*Kagan*, 2004; *Ogata and Katsura*, 2006]. It is obvious in Figures 2a, 2b, 2c, and 2d that the larger aftershocks begin early in the sequence, whereas the occurrence is progressively delayed for weaker events. To discuss c values, we need to consider only aftershocks having magnitudes greater than or equal to $m = m_c$. We discuss and apply several techniques to define the m_c values in section 4. Further, we point out that in the early period of an aftershock sequence ($0.001 < t$ (days) ≤ 0.01) the number of aftershocks was too small to provide good statistics of aftershock decay associated with the c value. Hence we consider the aftershock decay only for t (days) > 0.01.

3.5. Temporal Decay of Aftershock Activity

[26] To test the two hypotheses, we first need to show the observed time-dependent rate dN/dt for each sequence. For this test, dN/dt for different magnitude cutoffs m is required in order to study the scaling of τ with m in equation (3) and that of c with m in equation (5). In this work, discrete cutoffs (m_1, m_2, …, m_j, …, m_n) are considered and the difference in the cutoff $d_m = m_{j+1} - m_j$ is fixed to be 0.5. Figure 3 shows dN/dt as a function of t (days) for different cutoffs $m_1 = 2.0$, $m_2 = 2.5$, $m_3 = 3.0$, and $m_4 = 3.5$ for the Kobe earthquake. The rates dN/dt for $m_1 = 2.0$ in the time

Table 2. Comparison Between the Two Hypotheses for Several Values of the Side Length of the Space Window[a]

			Hypothesis I				Hypothesis II				
Side Length	b_T	A_T	p	c	MML_I	AIC_I	p	τ	MML_{II}	AIC_{II}	ΔAIC
					Kobe						
L + 10	0.749 (0.01)	4.69	1.20	0.304	269.000	−534.000	1.19	0.00135	302.408	−600.816	−66.816
L	0.739 (0.01)	4.64	1.22	0.359	300.263	−596.525	1.21	0.00146	334.765	−665.529	−69.004
L-10	0.735 (0.01)	4.6	1.24	0.324	462.838	−921.676	1.23	0.00129	494.848	−985.696	−64.020
L-20	0.727 (0.01)	4.57	1.25	0.302	465.886	−927.772	1.23	0.00180	495.625	−987.250	−59.478
L-30	0.722 (0.01)	4.54	1.25	0.260	452.971	−901.943	1.23	0.00108	481.975	−959.950	−58.007
					Tottori						
L + 10	0.799 (0.01)	4.92	1.22	0.045	1829.667	−3655.334	1.21	0.00106	1873.939	−3747.878	−92.544
L	0.799 (0.01)	4.92	1.22	0.423	1854.383	−3704.767	1.21	0.00104	1898.509	−3793.019	−88.252
L-10	0.798 (0.01)	4.91	1.22	0.419	1862.361	−3720.722	1.21	0.00105	1906.296	−3808.592	−87.870
L-20	0.797 (0.01)	4.89	1.25	0.436	2142.419	−4280.838	1.24	0.00101	2183.025	−4362.050	−81.212
L-30	0.796 (0.01)	4.89	1.25	0.423	2152.638	−4301.277	1.23	0.00097	2191.871	−4379.743	−78.466
					Niigata						
L + 5	0.636 (0.01)	4.68	1.40	1.268	3476.673	−6949.350	1.33	0.000944	3514.18	−7024.360	−75.010
L	0.677 (0.01)	4.77	1.40	1.200	3517.409	−7030.818	1.32	0.000926	3551.698	−7099.396	−68.578
L-5	0.670 (0.01)	4.75	1.41	1.250	3516.354	−7028.709	1.33	0.000944	3550.016	−7096.031	−67.322
L-10	0.675 (0.01)	4.77	1.39	1.120	3513.907	−7023.814	1.32	0.000895	3547.364	−7090.729	−66.915
L-15	0.635 (0.01)	4.65	1.41	1.141	3284.753	−6565.505	1.34	0.000904	3326.947	−6649.895	−84.390
					Fukuoka						
L + 10	0.746 (0.02)	4.66	1.30	0.241	1796.560	−3589.120	1.28	0.000750	1831.641	−3659.282	−70.162
L	0.746 (0.02)	4.66	1.30	0.241	1796.56	−3589.120	1.28	0.000750	1831.641	−3659.282	−70.162
L-10	0.746 (0.02)	4.66	1.30	0.241	1796.56	−3589.120	1.28	0.000750	1831.641	−3659.282	−70.162
L-20	0.739 (0.02)	4.64	1.30	0.230	1763.317	−3522.634	1.28	0.000729	1796.477	−3588.953	−66.319
L-30	0.731 (0.02)	4.60	1.30	0.206	1696.581	−3389.162	1.29	0.000700	1727.491	−3450.981	−61.819

[a]L shown in the column "side length" is given in Table 1. A_T and b_T: A and b values for aftershocks that occurred in the period (days) $0 < t < T$, where T is given in Table 1 and the value in parenthesis in the column "b_T" is the standard error. A set of p and c_0 is used for hypothesis I. Similarly, a pair of p and τ_0 is shown in hypothesis II. MLL_I and MLL_{II}: the maximum log-likelihood values for hypotheses I and II, respectively. AIC_I and AIC_{II}: the AIC values for hypothesis I and II, respectively. $\Delta AIC = AIC_{II} - AIC_I$.

window $0.01(=10^{-2.0}) < t$ (days) $\leq 1(=10^{0.0})$ and $m_2 = 2.5$ in the time window $0.01(=10^{-2.0}) < t$ (days) $\leq 0.32(=10^{-0.5})$ are not shown in Figure 3 and are also excluded from our hypotheses test. This is because these rates may partially reflect the effect of missing aftershocks, as discussed in section 4. The same plot has been performed for the other aftershock sequences: Tottori, in Figure 4, Niigata, in Figure 5, and Fukuoka, in Figure 6. It is generally seen that the observed decay curves are smoother for smaller m_j. The fluctuating curves for larger m_j can be attributed to poorer statistics.

4. Analysis of Aftershock Data Completeness

[27] The estimation of m_c is a difficult problem that requires a careful examination of the earthquake catalog. A review of various techniques used to determine m_c is given by *Wiemer and Wyss* [2002]. In this paper we adopt three frequently used methods to estimate m_c: the Maximum curvature (MAXC) method, the Goodness-of-Fit (GOF) method, and the entire-magnitude-range (EMR) method. Completeness magnitudes based on these methods are denoted by m_{cMAXC}, and m_{cGOF}, and m_{cEMR}, respectively. The final m_c value is chosen as the highest among these three.

4.1. MAXC Method

[28] This technique was proposed by *Wiemer and Wyss* [2000] and is less intensive computationally. The estimate of m_{cMAXC} is given by the point of maximum curvature of the frequency-magnitude distribution, which is determined using the local slope (i.e., the first derivative) of the frequency-magnitude curve. In practice m_{cMAXC} matches the magnitude bin with the highest frequency of events in the noncumulative frequency-magnitude distribution. Despite the ease of applicability and relative robustness of this approach, the m_{cMAXC} is often underestimated especially for gradually curved frequency-magnitude distributions that result from spatial or temporal heterogeneity.

4.2. GOF Method

[29] The GOF method compares observed and synthetic frequency-magnitude distributions to estimate the completeness magnitude [*Wiemer and Wyss*, 2000]. The m_{cGOF} value is determined in five steps: (1) Estimate the b and A values in equation (1) based on events with magnitudes greater than or equal to m_i, using the corrected maximum-likelihood estimate. (2) Compute a synthetic distribution of magnitudes with the same b, A, and m_i values. (3) Estimate the goodness of the fit, R, based on the computation of the absolute difference of the number of events in each magnitude bin assigned for m between the observed and the synthetic distributions. R is given by $R(b, A, m_i) = 100 - 100 \sum_{m=m_i}^{m_{UP}} |B(m) - S(m)| / \sum_{m=m_i}^{m_{UP}} B(m)$, where R takes a value in the range $0 \leq R \leq 100$, $B(m)$ and $S(m)$ are the observed and synthetic cumulative numbers of events in magnitude bin of m, respectively, and m_{UP} is the maximum value in the magnitude range of interest. For example, $R = 100$ means that there is no difference between the observed and synthetic distributions and $R = 90$ indicates that equation (1) with the assumed A and b values can explain 90% of the

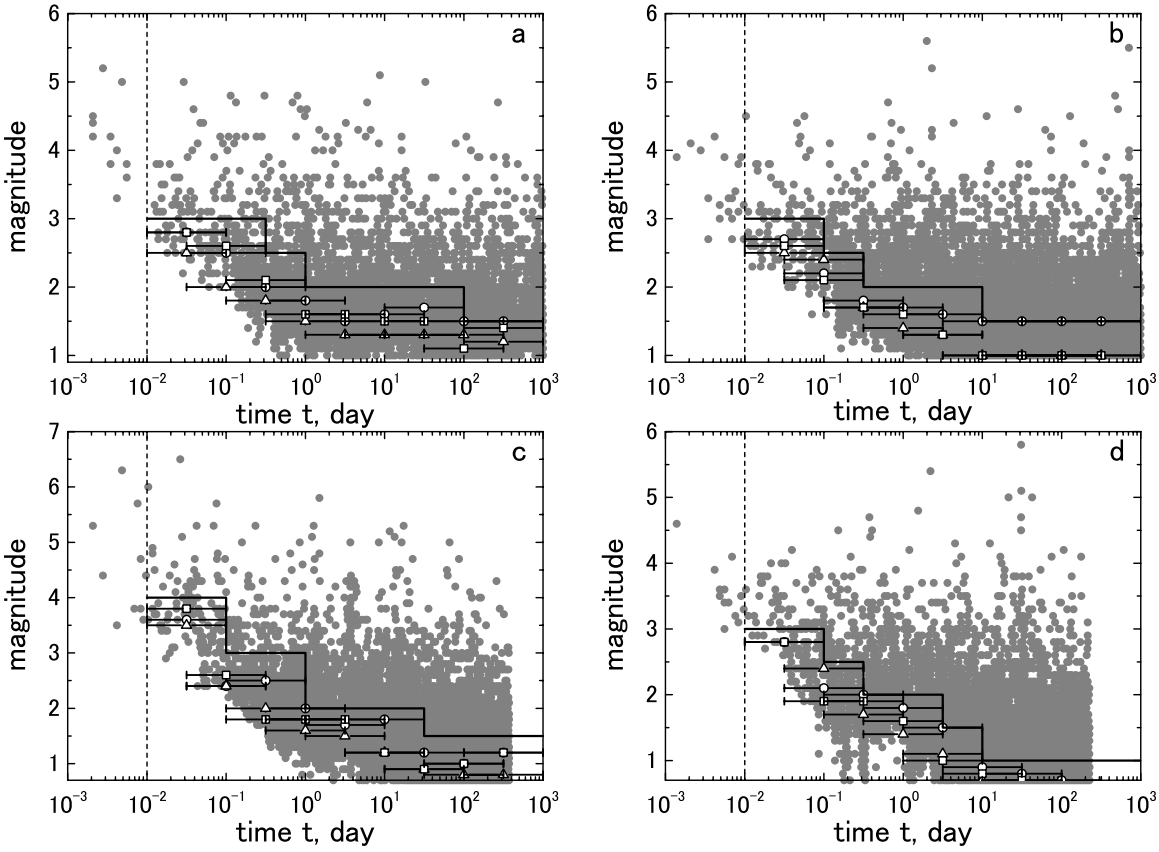

Figure 2. Time-magnitude distribution of aftershocks (circles) following the (a) Kobe, (b) Tottori, (c) Niigata, and (d) Fukuoka earthquakes. m_{cEMR} (circle), m_{cGOF} (triangle), and m_{cMAXC} (square) are also shown. These magnitudes are calculated using a time window: $\log_{10}T_{\mathrm{w}} < \log_{10}(t\ (\mathrm{days})) \leq \log_{10}T_{\mathrm{w}} + 1.0$, where T_{w} (days) = $10^{-2.0}$, $10^{-1.5}$, $10^{-1.0}$ ... The horizontal bars show the length of the window. Aftershocks that have magnitudes greater than or equal to a threshold (black curve) and occurred after the time t = 0.01 days (vertical dashed line) are used for our hypotheses test.

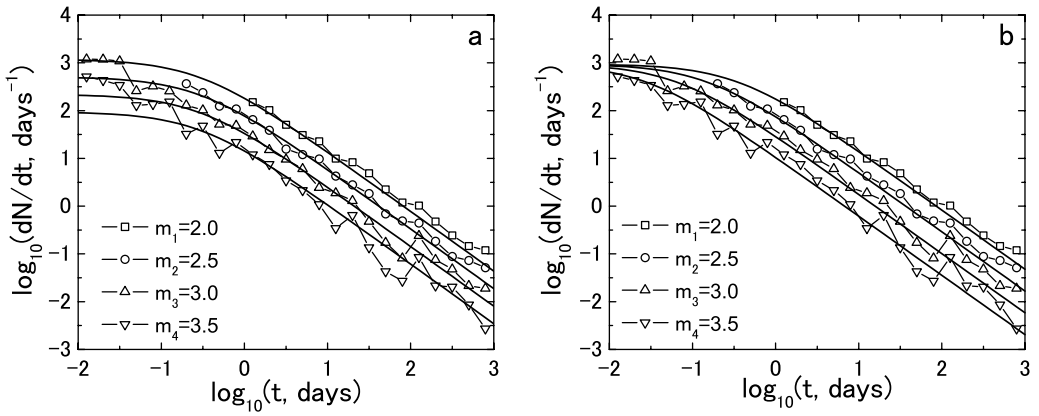

Figure 3. The decay of aftershock activity for the Kobe earthquake. We take the side length of the aftershock region to be L = 89 km. The rates of occurrence of aftershocks in number per day, dN/dt, are given for discrete cutoff magnitudes $m_1 = 2.0$ (square), $m_2 = 2.5$ (circle), $m_3 = 3.0$ (triangle), and $m_4 = 3.5$ (inverse triangle). The rates dN/dt of $m_1 = 2.0$ in $-2.0 \leq \log_{10}(t\ (\mathrm{days})) < 0.0$ and of $m_2 = 2.5$ in $-2.0 \leq \log_{10}(t\ (\mathrm{days})) < -0.5$ are not shown and included in our analysis, because the rate might involve the effect of missing aftershocks according to explanations in the text. (a) Hypothesis I and (b) Hypothesis II. c_0, τ_0, p, $\mathrm{AIC_I}$, $\mathrm{AIC_{II}}$, and ΔAIC are tabulated in Table 2. The predicted rates dN/dt drawn using these values are shown by curves.

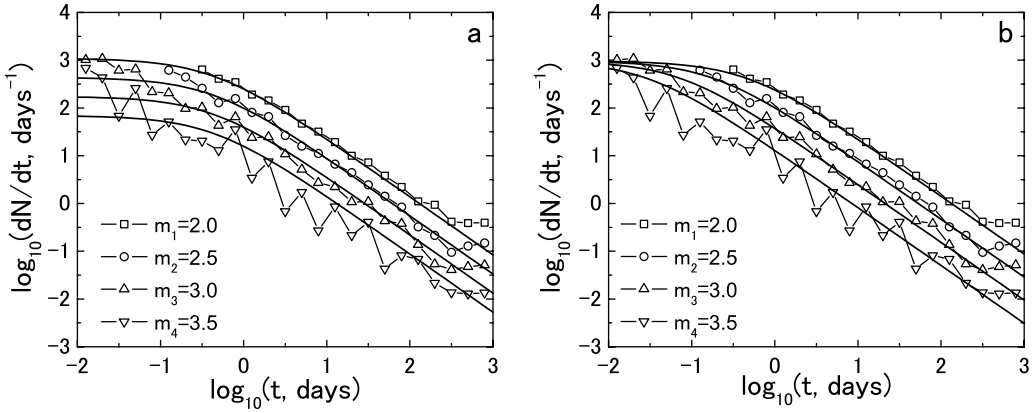

Figure 4. Dependence of dN/dt on t (days) for the Tottori aftershock sequence. The result for the linear extent L = 89 km is shown in this figure. (a) Hypothesis I and (b) Hypothesis II. See also the caption of Figure 3 for some explanation.

data variability for magnitudes greater than or equal to m_i. (4) Plot R as a function m_i. (5) Following *Wiemer and Wyss* [2000, 2002], define m_{cGOF} as the smallest m_i at which equation (1) can model 90% or more of the observed frequency-magnitude distribution. The 95% level of fit is rarely obtained for real catalogues; the 90% level is considered sufficient in most studies.

4.3. EMR Method

[30] This method was initially proposed by *Ogata and Katsura* [1993, 2006] who called it as the method combining the GR law with the detection rate function. In this study, following the modified version of *Woessner and Wiemer* [2005], we call the method as EMR and compute m_{cEMR}. The statistical modeling is done separately for the complete and the incomplete parts of the frequency-magnitude distribution. For aftershocks above a certain magnitude (m_{cc}), we assume the GR law behavior and compute b and A using the corrected maximum-likelihood estimate (see also section 3.3). For magnitudes smaller than m_{cc}, we hypothesize that the detection rate of aftershocks depends on their magnitudes in such a way that large aftershocks are almost entirely detected while smaller ones are detected at lower rates. In this method, the detection rate is assumed to be written as the cumulative function of the Normal distribution, $q = (\sigma\sqrt{2\pi})^{-1} \int_{-\infty}^{m_{cc}} \exp[-0.5(m-\mu)^2/\sigma]dm$ where μ and σ are constants. Here, μ is the magnitude at which 50% of the earthquakes are detected and σ denotes the standard deviation describing the width of the range where earthquakes are partially detected. Earthquakes with magnitudes greater than or equal to m_{cc} are assumed to be detected with a probability of one, q = 1. Here μ and σ are computed using the maximum-likelihood estimate. To evaluate the fit of the models with parameters (μ, σ, A, b), for various m_{cc}, to the data, we compute the log-likelihood, and plot it as a funnction of m_{cc}. The best fitting model is the one that maximizes the log-likelihood. *Woessner and Wiemer* [2005] compared this method with the GOF and MAXC techniques and show that the EMR method performs better when applied to synthetic and real data from regional and global earthquake catalogs. However, the EMR technique is most computationally intensive.

4.4. Estimation of m_c

[31] Several studies have shown that m_c decreases with time in the first few hours after major earthquakes [e.g., *Helmstetter et al.*, 2006; *Peng et al.*, 2007; *Enescu et al.*, 2007]. Moreover, mixing events with different m_c values

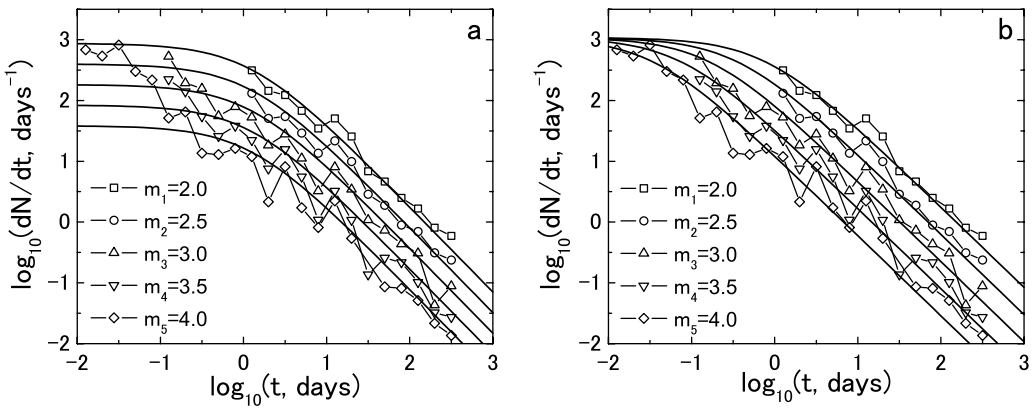

Figure 5. Dependence of dN/dt on t (days) for the Niigata aftershock sequence. We use a linear extent of L = 50 km. (a) Hypothesis I and (b) Hypothesis II. See also the caption of Figure 3 for some explanation.

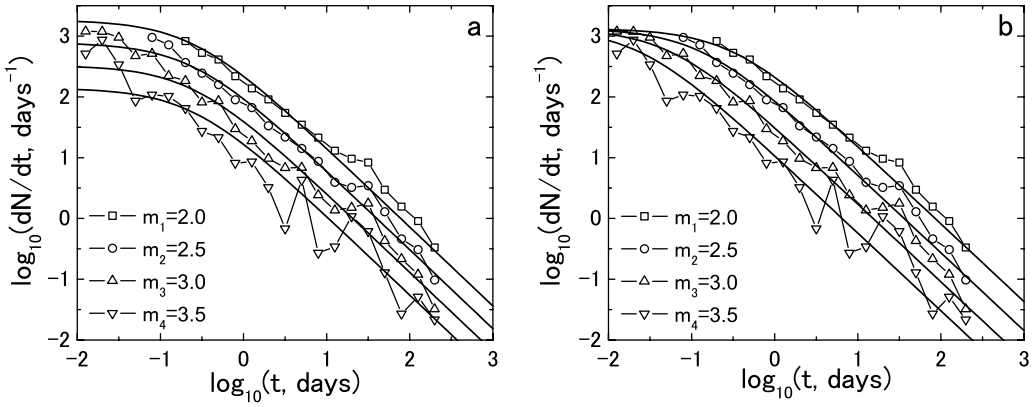

Figure 6. Dependence of dN/dt on t (days) for the Fukuoka earthquake. We take the side length of the space window to be $L = 63$ km. (a) Hypothesis I and (b) Hypothesis II. See also the caption of Figure 3 for some explanation for this figure.

would produce a biased frequency-magnitude distribution. Thus we determine m_c as a function of t (days), using a moving window approach. Here m_c is calculated for events in a window defined using the logarithm of its starting time ($\log_{10}T_w$): $\log_{10}T_w < \log_{10}(t) \leq \log_{10}T_w + 1.0$, where the window is moved by the change of T_w (days) = $10^{-2.0}$, $10^{-1.5}$, $10^{-1.0}$, ...

[32] We first apply the EMR, GOF, and MAXC techniques to the Kobe aftershock sequence. Figure 2a shows m_{cEMR}, m_{cGOF}, and m_{cMAXC} as a function of t by circles, triangles, and squares, respectively. The horizontal bars show the time windows in which aftershocks are used to compute the three magnitudes. In all cases, the completeness magnitude decreases with t in the early periods and reaches a constant value below 2.0. This time-dependent decrease is consistent with the data. We take m_c to be the largest value among the three magnitudes in each time window. The same analysis is done for the Tottori (Figure 2b), Niigata (Figure 2c), and Fukuoka (Figure 2d) earthquakes. The $t - m_c$ pattern observed for these events is similar with that observed for the Kobe case.

[33] On the basis of the $t - m_c$ pattern obtained above, we define a criterion to select the data for testing the two hypotheses of aftershock decay. In Figures 3–6, dN/dt is given as a function of t for discrete magnitude cutoffs (m_1, m_2, ..., m_j, ..., m_n). If m_1, m_2, ..., m_j are smaller than m_c, dN/dt for these cutoffs might be influenced by the effect of missing aftershocks. Thus only the rates dN/dt for m_{j+1}, m_{j+2}, ..., m_n ($\geq m_c$) should be considered for the test. Consequently, we use only aftershocks having magnitudes greater than or equal to a threshold = m_{j+1}.

[34] We first apply this criterion to the Kobe sequence. In this case, based on the $t - m_c$ pattern in Figure 2a, dN/dt for $m_1 = 2.0$ in the period $-2.0 < \log_{10}t \leq 0.0$ is not considered because $m_1 < m_c$ in this period. Similarly, we do not take into account dN/dt for $m_2 = 2.5$ in $-2.0 < \log_{10}t \leq -0.5$. In contrast, dN/dt for $m_3 = 3.0$ and $m_4 = 3.5$ is considered for the whole period $-2.0 < \log_{10}t \leq 3.0$. Thus we use aftershocks having magnitudes greater than or equal to thresholds (curve in Figure 2a) that are equal to $m_3 = 3.0$ for $-2.0 < \log_{10}t \leq -0.5$, $m_2 = 2.5$ for $-0.5 < \log_{10}t \leq 0.0$, and $m_1 = 2.0$ for $0.0 < \log_{10}t \leq 3.0$. The lower bound of magnitudes of used aftershocks is shown by curve in this figure. The same criterion has been applied to the other aftershock sequences: Figures 2b and 4 for the Tottori, Figures 2c and 5 for the Niigata, and Figures 2d and 6 for the Fukuoka. On the basis of the aftershock data defined here, the test is carried out using an objective statistical measure that is outlined below.

5. Point Process Modeling, Maximum Likelihood Method, and AIC

[35] To choose the best hypothesis between I and II, we need to find the best fit to the data for each hypothesis and then compare between them. To objectively find the best fit, a quantitative method to measure the goodness-of-fit is necessary. For this purpose, we do a statistical analysis called "point process modeling," which is often used for time series analysis of earthquakes [e.g., *Ogata*, 1983, 1999; *Guo and Ogata*, 1997].

5.1. Point Process Modeling

[36] In order to do the modeling we first need to define the intensity function λ. To find the best fit of model curves to observed curves for different cutoffs (m_1, m_2, ..., m_j, ..., m_n), λ is given as the occurrence rate of aftershocks with magnitudes from m_j to $m_{j+1}(=m_j + d_m)$, where $d_m = 0.5$ in this study. We obtain $\lambda(t, m_j) = \tau_1^{-1}(1 + t/c_1)^{-p} - \tau_2^{-1}(1 + t/c_2)^{-p}$, where the times τ_1, τ_2, c_1, and c_2 are defined for the individual hypotheses as follows. The hypothesis I: τ_1 and $\tau_2 = \tau(m)$ in equation (3) with $m = m_j$ and m_{j+1}, respectively, and $c_1 = c_2 = c_0$. The hypothesis II: c_1 and $c_2 = c(m)$ in equation (5) with $m = m_j$ and m_{j+1}, respectively, and $\tau_1 = \tau_2 = \tau_0$. Note that λ shows the occurrence rate of aftershocks with magnitudes from m_j to m_{j+1}. Thus we do not assume constant magnitudes between m_j and m_{j+1}.

[37] We next calculate the log-likelihood $\ln(L(m_j))$ for a point process model of aftershocks of magnitudes from m_j to m_{j+1}. This can be obtained as follows,

$$\ln\left(L\left(m_j\right)\right) = \sum_q \ln\left(\lambda\left(t_q, m_j\right)\right) - \int_{S_{m_j}}^{T} \lambda\left(t, m_j\right) dt, \qquad (7)$$

where $\{t_q: q = 1, 2, \ldots\}$ are the occurrence times of aftershocks of magnitudes from m_j to m_{j+1} in a monitored

time period $[S_{m_j}, T]$. Note that S_{m_j} is dependent on m_j while T is not. We take the dependence of S_{m_j} on m_j to exclude aftershocks in a time window where some aftershocks with magnitudes larger than or equal to m_j are interpreted to be missing before the time S_{m_j}.

[38] Using $\ln(L(m_j))$, we define the cumulative log-likelihood $\ln(L_{\mathrm{like}})$ for magnitudes from m_1 to m_n: $\ln(L_{\mathrm{like}}) \equiv \ln(L(m_1)) + \ln(L(m_2)) + \ldots + \ln(L(m_{n-1}))$. Suitable values of parameters maximize $\ln(L_{\mathrm{like}})$ and provide the best fitting to the data. In our case, the corresponding parameters are p and c_0 for hypothesis I and p and τ_0 for hypothesis II. The maximum log-likelihood is denoted by MLL (MLL_{I} for hypothesis I and MLL_{II} for hypothesis II).

[39] The reader may note that previous studies [e.g., *Ogata*, 1983, 1999; *Guo and Ogata*, 1997] take the form of λ to be similar to equation (2). This conventional form is not the same as that defined above and is not applicable to our case. If this form is used to obtain $\ln(L(m_j))$, large earthquakes would be included multiple times into the calculation of $\ln(L_{\mathrm{like}})$: for example, earthquakes with magnitudes larger than m_2 and smaller than m_3 would be included into the computation of both $\ln(L(m_1))$ and $\ln(L(m_2))$. To avoid this, we use $\lambda(t, m_j) = \tau_1^{-1}(1 + t/c_1)^{-p} - \tau_2^{-1}(1 + t/c_2)^{-p}$.

5.2. AIC

[40] Our primary criterion of model selection is based on the visual comparison between the best fits for hypotheses I and II. To support this point, we provide a test using the Akaike Information Criterion (AIC) [*Akaike*, 1974].

[41] The statistic $\mathrm{AIC} = -2MLL + 2n_{\mathrm{p}}$ is computed for each of the models fitted to the same data, where n_{p} is the total number of fitted parameters. In general, for comparing models with different numbers of parameters, the addition of the quantity $2n_{\mathrm{p}}$ roughly compensates for the flexibility which the extra parameters provide. For our research, n_{p} for the models of hypotheses I and II is 2: there is no difference in n_{p} between these models. The model with lower AIC-value is considered the better choice.

[42] Because it depends on the likelihood ratio, AIC can also be used as a rough guide for model testing. When we test a model with $n_{\mathrm{p}} + d_{\mathrm{np}}$ parameters against a null hypothesis with just n_{p} parameters (d_{np} is the difference in number of parameters) and these are nested subset models (for example, a linear model with different number of parameters), then a difference of 2 in AIC ($\Delta\mathrm{AIC} = 2$) is a rough estimate of significance at the 5% level [see *Hainzl and Ogata*, 2005]. Thus if the absolute value of ΔAIC is larger than 2 ($|\Delta\mathrm{AIC}| > 2$), the difference in goodness of fit between one model and the other is significant. However, models of hypotheses I and II are not nested. In such case, as a rule of thumb, $|\Delta\mathrm{AIC}| = 9.22$ is a rough estimate of significance at the 1% level [*Kalbfleisch and Prentice*, 1980]. In the present paper, we define $\Delta\mathrm{AIC} \equiv \mathrm{AIC}_{\mathrm{II}} - \mathrm{AIC}_{\mathrm{I}}$, where $\mathrm{AIC}_{\mathrm{I}}$ and $\mathrm{AIC}_{\mathrm{II}}$ are AIC values for the models of hypotheses I and II and use this rough indication to support our visual comparison.

6. Comparison Between the Two Hypotheses

[43] We first analyze the Kobe aftershock sequence, for the side length of $L = 89$ km. We take $A_{\mathrm{T}} = 4.64$ and $b_{\mathrm{T}} = 0.74$, magnitude cutoffs $m_1 = 2.0$, $m_2 = 2.5$, $m_3 = 3.0$, and $m_4 = 3.5$, starting times (days) $S_{m_1} = 10^{0.0}$, $S_{m_2} = 10^{-0.5}$, and $S_{m_3} = 10^{-2.0}$, and ending times (days) $T = 10^3$. For the model of hypothesis I, the pair of $c_0 = 0.359$ (days) and $p = 1.22$ gives $MML_{\mathrm{I}} = 300.263$ (Table 2). For the secondary hypothesis, the pair of $\tau_0 = 0.00146$ (days) and $p = 1.21$ gives $MML_{\mathrm{II}} = 334.765$ (Table 2). Using these parameter values, we show in Figures 3a and 3b the predictions for the dependence of dN/dt on t (days) for the models of hypotheses I and II, respectively. In the time interval (days) $-1.0 < \log_{10}(t) \leq 3.0$, the predicted rates based on both models are similar and also in good agreement with the observed rates. However, in the early time period $-2.0 < \log_{10}(t) \leq -1.0$, the predicted rates for hypothesis I significantly deviate from the observed rates, while no large deviation is found for the competing hypothesis II. Therefore the model of hypothesis II is considered to be better than that of hypothesis I.

[44] To support our visual comparison, we check the AIC values: $\mathrm{AIC}_{\mathrm{I}} = -596.525$, $\mathrm{AIC}_{\mathrm{II}} = -665.529$, and $\Delta\mathrm{AIC} = -69.004$ (Table 2). We find that $\mathrm{AIC}_{\mathrm{I}}$ is larger than $\mathrm{AIC}_{\mathrm{II}}$ and ΔAIC is clearly less than -9.22. These values show that hypothesis II gives a significantly better representation of the observed data than hypothesis I. Thus on the basis of this AIC test, we support hypothesis II, a constant $\tau = \tau_0$ and the scaling of c with m.

[45] We also suggest that the difference in predicted rates for the early period $-2.0 < \log_{10}(t) \leq -1.0$ between hypothesis I (Figure 3a) and hypothesis II (Figure 3b) is associated with $\Delta\mathrm{AIC} = -69.004$, whose absolute value is significantly larger than 9.22. We would like to emphasize here that the difference between the two models for the early part of an aftershock sequence is very unlikely to have been caused by catalog incompleteness since only aftershocks with magnitudes greater than or equal to m_{c} have been used.

[46] The above results are robust and do not change significantly when the side length of the spatial window is varied from the used value L(=89 km). To test this, we considered several values for the side length: $L + 10$(=99 km), $L - 10$(=79 km), $L - 20$(=69 km), and $L - 30$(=59 km). The obtained parameter values are summarized in Table 2. Using the parameters A_{T}, b_{T}, p, c_0, and τ_0, we reproduced the predicted rates for hypothesis I and II. We found for all the cases that the predicted rates for hypothesis I significantly deviate from the observed rates for the period $-2.0 < \log_{10} t \leq -1.0$ in contrast to a significantly smaller deviation for hypothesis II. This shows that hypothesis II is better than hypothesis I. Moreover, comparison between $\mathrm{AIC}_{\mathrm{I}}$ and $\mathrm{AIC}_{\mathrm{II}}$ supports the model of hypothesis II rather than the model of hypothesis I. The same analysis has been performed for the other three cases. The obtained parameter values are tabulated in Table 2. Figures 4–6 show the results for the cases of Tottori, Niigata, and Fukuoka aftershock sequences, respectively. The linear extent of aftershock region is taken to be L. On the basis of visual inspection and calculated AIC values, we found similar results as for the Kobe aftershock sequence. Thus we conclude that hypothesis II is significantly better than hypothesis I in quantifying the decay of aftershock activity for the Japanese earthquakes studied here, and constant $\tau = \tau_0$ and the scaling of c with m are good approximations.

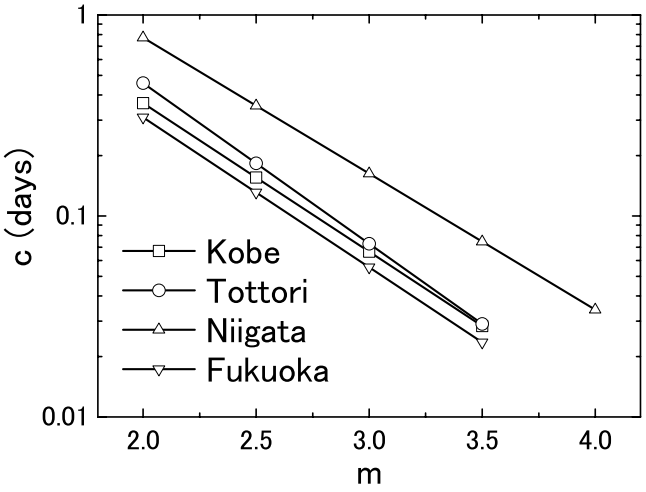

Figure 7. Dependence of c (days) on m for the Kobe (square), Tottori (circle), Niigata (triangle), and Fukuoka (inverse triangle) aftershock sequences. We take the side length of aftershock region to be L.

This scaling for the four earthquakes is given in Figure 7 taking the linear extent to be L.

7. Discussion and Conclusions

[47] We modified the approach of *Shcherbakov et al.* [2004, 2005, 2006], combining equations (1) and (2). As a result, we reformulated the scaling of c with m in equations (5) and (6) assuming that τ is a constant independent on m (hypothesis II). We also found alternative scaling of τ with m in equations (3) and (4) under the assumption of constant c independent on m (hypothesis I). We investigated whether these forms well approximate the temporal decay of aftershocks for the Japanese earthquakes and which is better for approximating the decay.

[48] We applied three existing techniques for determining m_c. Then m_c in this paper was defined as the largest value among the three. For all the analyzed sequences, m_c decreases with time immediately after the mainshock and reaches a constant value at later times (Figure 2). Only events with magnitudes greater than or equal to m_c were used for our analysis. For each of the two models of hypotheses I and II, we used point process modeling and a maximum likelihood method to find the best fit to the data. We also introduced AIC as a significance measure of the difference between the two competing models. Our analysis provides support for the model of hypothesis II, and the present conclusion is consistent with that obtained by previous studies [*Shcherbakov et al.*, 2004, 2005, 2006]. We also checked whether or not this conclusion is changed by varying the spatial extent of aftershock region but found no significant change.

[49] We further discuss the predicted rates dN/dt for hypothesis II as shown in Figures 3b, 4b, 5b, and 6b. It is noticed that these rates are slightly different for different cutoff magnitudes (m_1, m_2, ..., m_j, ..., m_n), immediately after a mainshock. After the time $c(m_j)$, the equal spacing between the theoretical curves for m_j, m_{j+1},..., m_n is valid. That is, there is the characteristic time $c(m)$ required for starting a power law decay and this time is decreasing for increasing m. This result shows that there are fewer aftershocks than predicted by a power law rate decay immediately after a mainshock and that this aftershock deficit can be seen for longer times at lower threshold magnitudes.

[50] It is of interest to discuss the mechanism of aftershocks based on our results. We relate this mechanism to time delays associated with brittle failure and explore it from the viewpoint of damage mechanics. Some parts of damage mechanics for the deformation of a brittle solid are still quasi-empirical. However, the constitutive equations used for the dependence of rate of damage generation on strain ε and stress σ have a thermodynamic basis [*Kachanov*, 1986; *Krajcinovic*, 1996; *Lyakhovsky et al.*, 1997]. The behavior of a stressed brittle solid is metastable, and statistical variation of times required to nucleate microcracks is described according to the sample's state specified by ε and σ. We see the analogy between the aftershock decay according to hypothesis II and the predicted decay using a damage mechanics model. On the basis of this analogy, it is argued that aftershocks are the earthquakes that it takes time to nucleate.

[51] Damage refers to irreversible deformation of solids. Some examples include plasticity, brittle microcracking, and thermally activated creep [*Krajcinovic*, 1996]. In order to quantify the damage evolution associated with microcracking, several models were introduced in civil and mechanical engineering [e.g., *Kachanov*, 1986; *Krajcinovic*, 1996] and have also been applied to the brittle deformation of the Earth's crust [e.g., *Lyakhovsky et al.*, 1997; *Ben-Zion and Lyakhovsky*, 2006; *Shcherbakov et al.*, 2005]. *Shcherbakov and Turcotte* [2003, 2004] used the concept of the yield stress σ_y and the corresponding yield strain ε_y for the damage evolution where $\varepsilon_y = \sigma_y/E_0$ with the Young's modulus E_0. Damage occurs in the form of microcracking at stresses greater than the yield stress ($\sigma > \sigma_y$). Below this stress ($\sigma \leq \sigma_y$) no damage occurs. Using the constitutive equation with the yield parameters, *Nanjo et al.* [2005] considered a viscoelastic damage model and derived the modified Omori's law in equation (2). Their working hypotheses are (1) the stress transfer during a main shock increases the stress and strain above the yield values in some regions adjacent to the fault on which the mainshock occurred, (2) the increases of stress and strain are essentially instantaneous and follow linear elasticity, and the increased stress σ_0 and strain ε_0 satisfy $\sigma_0 = \varepsilon_0 E_0$, and (3) the applied strain remains constant ($\varepsilon = \varepsilon_0$) and aftershocks relax the stress from the initial value σ_0 to the yield value σ_y. They showed that this stress relaxation can reproduce equation (2) and that the logarithm of the c value is inversely proportional to the excess stress $\sigma_0 - \sigma_y = E_0(\varepsilon_0 - \varepsilon_y)$ [see *Nanjo et al.*, 2005, equation (34)]. It is reasonable to assume that the large aftershocks occur in regions where the instantaneous stress (strain) transfer from the mainshock is large (large excess stress). This can be attributed to the association between higher stress (strain) levels and larger aftershocks. The damage mechanics approach shows the inverse dependence of the c value on the magnitude of aftershocks. We see a close association of aftershock decay predicted using the damage model with the aftershock decay obtained in this study (hypothesis II). Thus on the basis of this association, we propose that the time delay of the after-

shocks relative to the mainshock is in direct analogy to the time delay of the damage. This delay is because it takes time to nucleate microcracks (aftershocks). Similar discussions were given by *Shcherbakov and Turcotte* [2003, 2004] and *Shcherbakov et al.* [2005] but they did not discuss from the viewpoint of the *c* value.

[52] Other studies also suggest that the time delays associated with aftershocks are analogous to times required to nucleate microcracks. This analogy was first proposed by *Mogi* [1962] who studied aftershocks accompanying earthquakes in and near Japan and rock fracture experiments. The recent example is the attribution of the time delays associated with the nucleation and growth of a single crack to stress corrosion [*Freund*, 1990]. This explanation has been applied to the time delays associated with aftershocks following the original and modified Omori's law [*Das and Scholz*, 1981; *Yamashita and Knopoff*, 1987]. Another approach to the time delays is based on friction. Laboratory studies of friction between rock surfaces are empirically correlated with rate-and-state friction laws [*Dieterich*, 1978; *Ruina*, 1983]. When the slip velocity is changed there is a time delay associated with the establishment of a new steady-state coefficient of friction. The state variable in the friction law has also been used to quantify the delay in rupture on a frictional surface. *Dieterich* [1994] has derived the Omori's law for the time delays of earthquake aftershocks from the equations of rate-and-state friction. There is clearly a close association between these works and the damage mechanics approach.

[53] There is debate over the existence of *c* value (positive versus zero or negative) among researchers [e.g., *Narteau et al.*, 2002; *Kagan*, 2004; *Shcherbakov et al.*, 2004, 2005, 2006; *Gasperini and Lolli*, 2006; *Lolli and Gasperini*, 2006]. *Kagan* [2004] and *Ogata and Katsura* [2006] discussed the incomplete detection of small aftershocks at the beginning of an aftershock sequence. Their results imply that the value *c* was partially influenced by the effect of this incomplete detection. *Vidale et al.* [2003], *Peng et al.* [2006, 2007], and *Enescu et al.* [2007] used high-quality waveform data to show that immediately after the mainshock, small aftershocks are usually "masked" by the mainshock coda and not recorded in earthquake catalogs. These authors argue for a small, but nonzero *c* value. Although nonzero *c* values have been obtained for adequately observed and selected data, the increase of *c* with the decrease of *m* has been attributed to the lack of small magnitude events over short times [e.g., *Hamaguchi and Hasegawa*, 1970; *Eaton*, 1990; *Narteau et al.*, 2002]. We applied commonly accepted techniques to define m_c, below which small earthquakes might be missing from the catalog records [*Ogata and Katsura*, 1993, 2006; *Wiemer and Wyss*, 2000, 2002; *Woessner and Wiemer*, 2005]. Our results, which were obtained based on the fitting of the proposed models to complete aftershock data, prefer the scaling of *c* with decreasing magnitude. This demonstrates that the increase of *c* with the decrease of *m* cannot always be attributed to the effect of missing aftershocks at short times after the mainshock. The overall consistency between our prediction and the data shows that positive *c* is not caused by missing aftershocks but a true consequence of aftershock dynamics associated with damage evolution.

[54] Finally, we suggest that further investigation of our models would contribute to a better understanding of aftershock statistics. The comparison between hypotheses I and II only helps to determine which model fits better to the data. However as pointed out above, it does not say anything about the reliability of each model. In other words, if our proposed models do not satisfactorily work for fitting the data, the use of other models becomes necessary. One of the possible alternatives is the Epidemic Type Aftershock Sequence (ETAS) model [e.g., *Guo and Ogata*, 1997; *Ogata*, 1999; *Helmstetter et al.*, 2005; *Hainzl and Ogata*, 2005]. Thus it is of interest to understand how this model compares with the models of hypotheses I and II.

[55] **Acknowledgments.** The discussions with S. Wiemer, S. Hainzl, J. Zhuang, S. Toda, J. Mori, Y. Ben-Zion, D. Vere-Jones, J. H. Dieterich, and R. P. Schoenberg were very useful during the elaboration of this work. Suggestions by the Editor (R. Arculus) and the Associate Editor (R. Console) and reviews by Z. Peng and three anonymous referees have been very helpful in revising our manuscript. We thank JMA for providing earthquake data. This work is supported by the National Science Foundation (USA) under grant NSF ATM-03-27571 (DLT, RS); NASA/JPL grant 1247848 (RS); JSPS Research Fellowship (BE, KZN); EC-FP6-Project SAFER contract 036935 (BE, KZN), EC-Project NERIES contract 026130 (BE, KZN), Grant-in-Aid for Scientific Research 17200021, the Ministry of Education, Culture, Sport, Science and Technology (YO, TI); and Transdisciplinary Research Integration Center, Research Organization of Information and Systems (YO, TI). This paper is contribution number 1502 of the Geophysical Institute, ETHZ.

References

Akaike, H. (1974), A new look at the statistical model identification, *IEEE Trans. Autom. Control*, *19*, 716–723.

Aki, K. (1965), Maximum likelihood estimate of b in the formula logN = a-bM and its confidence limits, *Bull. Earthquake Res. Inst. Univ. Tokyo*, *43*, 237–239.

Båth, M. (1965), Lateral inhomogeneities in the upper mantle, *Tectonophysics*, *2*, 483–514.

Ben-Zion, Y., and V. Lyakhovsky (2006), Analysis of aftershocks in a lithospheric model with seismogenic zone governed by damage rheology, *Geophys. J. Int.*, *165*(1), 197–210, doi:10.1111/j.1365-246X.2006.02878.x.

Console, R., A. M. Lombardi, M. Murru, and D. Rhoades (2003), Båth's law and the self-similarity of earthquakes, *J. Geophys. Res.*, *108*(B2), 2128, doi:10.1029/2001JB001651.

Das, S., and C. H. Scholz (1981), Theory of time-dependent rupture in the Earth, *J. Geophys. Res.*, *86*, 6039–6051.

Dieterich, J. H. (1978), Time-dependent friction and the mechanics of stick-slip, *Pure Appl. Geophys.*, *116*, 790–806.

Dieterich, J. H. (1994), A constitutive law for rate of earthquake production and its application to earthquake clustering, *J. Geophys. Res.*, *99*, 2601–2618.

Eaton, J. P. (1990), The earthquake and its aftershocks from May 2 through September 30, 1983, in *The Coalinga, California, Earthquake of May 2, 1983*, edited by M. J. Rymer and W. L. Ellsworth, *U.S. Geol. Surv. Prof. Pap.*, *1487*, 113–170.

Enescu, B., and K. Ito (2002), Spatial analysis of the frequency-magnitude distribution and decay rate of aftershock activity of the 2000 Western Tottori earthquake, *Earth Planets Space*, *54*, 847–859.

Enescu, B., J. Mori, and M. Miyazawa (2007), Quantifying early aftershock activity of the 2004 mid-Niigata Prefecture earthquake (Mw6.6), *J. Geophys. Res.*, *112*, B04310, doi:10.1029/2006JB004629.

Freund, L. B. (1990), *Dynamic Fracture Mechanics*, 563 pp., Cambridge Univ. Press, Cambridge, U. K.

Gasperini, P., and B. Lolli (2006), Correlation between the parameters of the aftershock rate equation: Implications for the forecasting of future sequences, *Phys. Earth Planet. Int.*, *156*, 41–58.

Gross, S. J., and C. Kisslinger (1994), Tests of models of aftershock decay, *Bull. Seismol. Soc. Am.*, *84*, 1571–1579.

Guo, Z., and Y. Ogata (1997), Statistical relations between the parameters of aftershocks in time, space and magnitude, *J. Geophys. Res.*, *102*, 2857–2873.

Gutenberg, B., and C. F. Richter (1954), *Seismicity of the Earth and Associated Phenomena*, 2nd ed., 310 pp., Princeton Univ. Press, Princeton, N. J.

Hainzl, S., and Y. Ogata (2005), Detecting fluid signals in seismicity data though statistical earthquake modeling, *J. Geophys. Res.*, *110*, B05S07, doi:10.1029/2004JB003247.

Hamaguchi, H., and A. Hasegawa (1970), An investigation on the aftershocks of the Tokachi-oki earthquake of 1968, (2) Statistical study on time distribution, *Sci. Rep. Tohoku Univ. Ser. 5*, *20*, 119–130.

Helmstetter, A., and D. Sornette (2003), Båth's law derived from the Gutenberg-Richter law and from aftershock properties, *Geophys. Res. Lett.*, *30*(20), 2069, doi:10.1029/2003GL018186.

Helmstetter, A., Y. Kagan, and D. Jackson (2005), Importance of small earthquakes for stress transfers and earthquake triggering, *J. Geophys. Res.*, *110*, B05S08, doi:10.1029/2004JB003286.

Helmstetter, A., Y. Kagan, and D. D. Jackson (2006), Comparison of short-term and long-term earthquake forecast models for southern California, *Bull. Seismol. Soc. Am.*, *76*(1), 90–106.

Kachanov, L. M. (1986), *Introduction to Continuum Damage Mechanics*, 135 pp., Martinus Nijhoff, Dordrecht, Netherlands.

Kagan, Y. Y. (2002), Aftershock zone scaling, *Bull. Seismol. Soc. Am.*, *92*, 641–655.

Kagan, Y. Y. (2004), Short-term properties of earthquake catalogs and models of earthquake source, *Bull. Seismol. Soc. Am.*, *94*, 1207–1228.

Kalbfleisch, J. D., and R. L. Prentice (1980), *The Statistical Analysis of Failure Time Data*, 321 pp., John Wiley, New York.

Kisslinger, C., and L. M. Jones (1991), Properties of aftershock sequences in southern California, *J. Geophys. Res.*, *96*, 11,947–11,958.

Krajcinovic, D. (1996), *Damage Mechanics*, 761 pp., Elsevier, Amsterdam.

Lolli, B., and P. Gasperini (2006), Comparing different models of aftershock rate decay: The role of catalog incompleteness in the first times after mainshock, *Tectonophysics*, *423*, 43–59.

Lyakhovsky, V., Y. Ben-Zion, and A. Agnon (1997), Distributed damage, faulting, and friction, *J. Geophys. Res.*, *102*, 27,635–27,649.

Marzocchi, W., and L. Sandri (2003), A review and new insights on the estimation of the *b*-value and its uncertainty, *Ann. Geophys.*, *46*, 1271–1282.

Mogi, K. (1962), On the time distribution of aftershocks accompanying the recent major earthquakes in and near Japan, *Bull. Earthquake Res. Inst. Univ. Tokyo*, *40*, 107–124.

Nanjo, K. Z., D. L. Turcotte, and R. Shcherbakov (2005), A model of damage mechanics for the deformation of the continental crust, *J. Geophys. Res.*, *110*(B7), B07403, doi:10.1029/2004JB003438.

Narteau, C., P. Shebalin, and M. Holschneider (2002), Temporal limits of the power law aftershock decay rate, *J. Geophys. Res.*, *107*(B12), 2359, doi:10.1029/2002JB001868.

Ogata, Y. (1983), Estimation of the parameters in the modified Omori formula for aftershock frequencies by the maximum likelihood procedure, *J. Phys. Earth*, *31*, 115–124.

Ogata, Y. (1999), Seismicity analysis through point-process modeling: A review, *Pure Appl. Geophys.*, *155*, 471–507.

Ogata, Y., and K. Katsura (1993), Analysis of temporal and spatial heterogeneity of magnitude frequency distribution inferred from earthquake catalogs, *Geophys. J. Int.*, *113*, 727–738.

Ogata, Y., and K. Katsura (2006), Immediate and updated forecasting of aftershock hazard, *Geophys. Res. Lett.*, *33*, L10305, doi:10.1029/2006GL025888.

Omori, F. (1894), On the after-shocks of earthquakes, *J. Colloid Sci.*, *7*, 111–200.

Peng, Z., J. E. Vidale, and H. Houston (2006), Anomalous early aftershock decay rates of the 2004 M6 Parkfield earthquake, *Geophys. Res. Lett.*, *33*, L17307, doi:10.1029/2006GL026744.

Peng, Z. G., J. E. Vidale, M. Ishii, and A. Helmstetter (2007), Seismicity rate immediately before and after main shock rupture from high-frequency waveforms in Japan, *J. Geophys. Res.*, *112*, B03306, doi:10.1029/2006JB004386.

Ruina, A. L. (1983), Slip instability and state variable friction laws, *J. Geophys. Res.*, *88*, 10,359–10,370.

Scordilis, E. M. (2005), Globally valid relations converting M_S, m_b and M_{JMA} to M_W, in *Book of Abstracts of NATO Advanced Research Workshop, Earthquake Monitoring and Seismic Hazard Mitigation in Balkan Countries (Borovetz, Bulgaria, September 11–17, 2005)*, edited by E. S. Husebye and C. Christova, pp. 158–161, Kamea Ltd., Sofia.

Shcherbakov, R., and D. L. Turcotte (2003), Damage and self-similarity in fracture, *Theor. Appl. Frac. Mech.*, *39*, 245–258.

Shcherbakov, R., and D. L. Turcotte (2004), A damage mechanics model for aftershocks, *Pure Appl. Geophys.*, *161*, 2379–2391.

Shcherbakov, R., D. L. Turcotte, and J. B. Rundle (2004), A generalized Omori's law for earthquake aftershock decay, *Geophys. Res. Lett.*, *31*, L11613, doi:10.1029/2004GL019808.

Shcherbakov, R., D. L. Turcotte, and J. B. Rundle (2005), Aftershock statistics, *Pure Appl. Geophys.*, *162*, 1051–1076, doi:10.1007/s00024-004-2661-8.

Shcherbakov, R., D. L. Turcotte, and J. B. Rundle (2006), Scaling properties of the Parkfield aftershock sequence, *Bull. Seismol. Soc. Am.*, *69*, S376–S384.

Shi, Y., and B. A. Bolt (1982), The standard error of the magnitude-frequency b-value, *Bull. Seismol. Soc. Am.*, *72*, 1677–1687.

Turcotte, D. L. (1997), *Fractals and Chaos in Geology and Geophysics*, 2nd ed., 412 pp., Cambridge Univ. Press, Cambridge, U. K.

Utsu, T. (1961), A statistical study on the occurrence of aftershocks, *Geophys. Mag.*, *30*, 521–605.

Utsu, T. (1962), On the nature of three Alaskan aftershock sequences of 1957 and 1958, *Bull. Seismol. Soc. Am.*, *52*, 279–297.

Utsu, T. (1969), Aftershocks and earthquake statistics (I): Source parameters which characterize an aftershock sequence and their interrelations, *J. Fac. Sci. Hokkaido Univ., Ser. 7*, *3*, 129–195.

Utsu, T., Y. Ogata, and R. S. Matsu'ura (1995), The centenary of the Omori formula for a decay law of aftershock activity, *J. Phys. Earth*, *43*, 1–33.

Vere-Jones, D. (1969), A note on the statistical interpretation of Båth's law, *Bull. Seismol. Soc. Am.*, *59*, 1535–1541.

Vere-Jones, D., J. Murakani, and A. Christophersen (2006), A further note on Bath's law, paper presented at the 4th International Workshop on Statistical Seismology (Statsei4), Inst. of Stat. Math., Tokyo.

Vidale, J. E., E. S. Cochran, H. Kanamori, and R. W. Clayton (2003), After the lightning and before the thunder: non-Omori behavior of early aftershocks?, *Eos Trans. AGU*, *84*(46), Fall Meet. Suppl., Abstract S31A-08.

Wiemer, S., and M. Wyss (2000), Minimum magnitude of complete reporting in earthquake catalogs: Examples from Alaska, the Western United States, and Japan, *Bull. Seismol. Soc. Am.*, *90*, 859–869.

Wiemer, S., and M. Wyss (2002), Mapping spatial variability of the frequency-magnitude distributions of earthquakes, *Adv. Geophys.*, *45*, 259–302.

Woessner, J., and S. Wiemer (2005), Assessing the quality of earthquake catalogues: Estimating the magnitude of completeness and its uncertainty, *Bull. Seismol. Soc. Am.*, *95*, 684–698, doi:10.1785/0120040007.

Yamashita, T., and L. Knopoff (1987), Model of aftershock occurrence, *Geophys. J. R. Astron. Soc.*, *91*, 13–26.

B. Enescu, Department 2 - Physics of the Earth, GeoForschungsZentrum, Telegrafenberg, D-14473 Potsdam, Germany. (benescu@gfz-potsdam.de)

T. Iwata and Y. Ogata, Institute of Statistical Mathematics, 4-6-7, Minami-Azabu, Minato-ku, Tokyo 106-8569, Japan. (iwata@ism.ac.jp; ogata@ism.ac.jp)

K. Z. Nanjo, Swiss Seismological Service, ETH Hönggerberg, HPP P, CH-8093 Zürich, Switzerland. (nanjo@sed.ethz.ch)

R. Shcherbakov, Center for Computational Science and Engineering, University of California, Davis, One Shields Avenue, Davis, CA 95616, USA. (roshch@cse.ucdavis.edu)

D. L. Turcotte, Department of Geology, University of California, Davis, One Shields Avenue, Davis, CA 95616, USA. (turcotte@geology.ucdavis.edu)